Multivalent Ion-Mediated Attraction between Like-Charged Colloidal Particles: Nonmonotonic Dependence on the Particle Charge

Cheng Lin, Xiaowei Qiang, Hai-Long Dong, Jie Huo,* and Zhi-Jie Tan*

Cite This: *ACS Omega* 2021, 6, 9876–9886

Read Online

ACCESS | Metrics & More | Article Recommendations | Supporting Information

ABSTRACT: Ion-mediated effective interactions are important for the structure and stability of charged particles such as colloids and nucleic acids. It has been known that the intrinsic electrostatic repulsion between like-charged particles can be modulated into effective attraction by multivalent ions. In this work, we examined the dependence of multivalent ion-mediated attraction between like-charged colloidal particles on the particle charge in a wide range by extensive Monte Carlo simulations. Our calculations show that for both divalent and trivalent salts, the effective attraction between like-charged colloidal particles becomes stronger with the increase of the particle charge, whereas it gradually becomes weakened when the particle charge exceeds a "critical" value. Correspondingly, as the particle charge is increased, the driving force for such effective attraction transits from an attractive electrostatic force to an attractive depletion force, and the attraction weakening by high particle charges is attributed to the transition of electrostatic force from attraction to repulsion. Our analyses suggest that the attractive depletion force and the repulsive electrostatic force at high particle charges result from the Coulomb depletion which suppresses the counterion condensation in the limited region between two like-charged colloidal particles. Moreover, our extensive calculations indicate that the "critical" particle charge decreases apparently for larger ions and smaller colloidal particles due to stronger Coulomb depletion and decreases slightly at higher salt concentrations due to the slightly enhanced Coulomb depletion in the intervening space between colloidal particles. Encouragingly, we derived an analytical formula for the "critical" particle charge based on the Lindemann melting law.
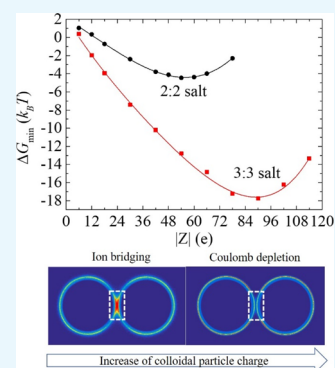
1. INTRODUCTION

Ion-mediated interactions between charged particles are critical to the structure assembly, complexation, and stability of colloids, nucleic acids, and proteins due to their polyelectrolyte nature.[1-11] For over 2 decades, the effective interactions between like-charged particles have drawn rather considerable interest given that they are strongly coupled to many important processes in biology and physics such as colloid structure stability and nucleic acid structure assembly.[12-25] Early on, classical models in the framework of mean-field theories such as the Poisson−Boltzmann theory have been widely employed to study the effective interactions between charged particles in electrolyte solutions.[26-28] However, despite their great success, those mean-field-based approaches failed for polyelectrolyte systems under certain salt conditions such as at a very high monovalent salt concentration and in the presence of a multivalent salt. This is attributed to the mean-field approximation that inter-ion correlations are intrinsically ignored since such inter-ion correlations can play a fundamental role in ion-mediated interactions between charged particles.[1,29-39]

Counterions can bind to charged particles and consequently modulate effective interactions between charged particles. Beyond the mean-field descriptions, for oppositely charged

particles, multivalent ions of a high concentration can modulate intrinsically Coulombic attractions into effective repulsions.[39-41] In parallel, for like-charged particles, multivalent ions can modulate intrinsically Coulombic repulsions into effective attractions, which could drive the condensation or aggregation of charged particles such as nucleic acids,[42-47] proteins,[48,49] and colloids.[50-62] The mechanisms for multivalent ion-mediated like-charge attractions are diverse and are attributed to counterion bridging,[50,58,61-64] depletion force,[52,63] and charge fluctuations of condensed counterions.[55,65-68] Alternatively, condensed counterions could be modeled as one component plasma around oppositely charged particles (voids), and the effective like-charge attraction could be attributed to a competition among the ion−ion and void−void repulsions and the ion−void attraction.[69] Recently, specific counterion configuration[70] and depletion[71] were
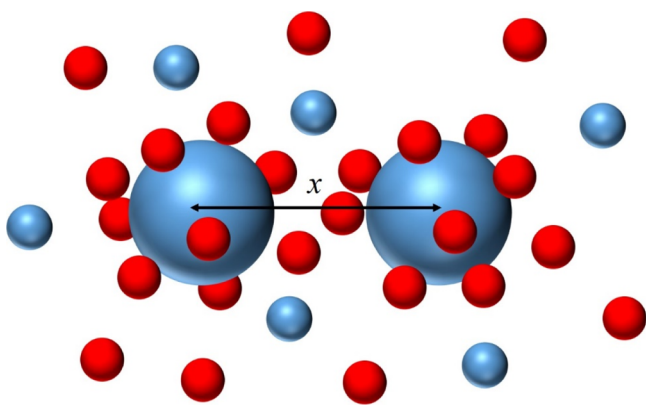
reported to be able to cause the like-charge attractions at high monovalent salt concentrations.

Furthermore, it has been shown that effective like-charge attractions are strongly dependent on particle charge structures,[15,72] competition between ions of different valences,[73] dielectric constants,[74,75] temperatures,[76] ion sizes,[77−82] and particle charge densities.[83−85] For example, recent experiments and simulations show that ion-mediated interactions between nucleic acids are dependent strongly on their helical structures.[44,47] Additionally, particles with a higher charge density would involve stronger ion−particle binding and consequently the multivalent ion-mediated like-charge attraction generally becomes stronger for higher particle charges.[83,84] However, until now, the covered range of particle charge densities is rather limited in previous works, thus it is still unclear how the multivalent ion-mediated attraction between like-charged particles depends on the particle charge in a wide range.[85]

In this work, we employed Monte Carlo simulations to calculate the potentials of mean force (PMFs) between two like-charged colloidal particles with a wide range of particle charges in symmetrical divalent and trivalent salt solutions and to explore how multivalent ion-mediated like-charge attraction depends on the particle charge. Our calculations show that the effective like-charge attraction is nonmonotonically dependent on the particle charge: with the increase of the particle charge, the effective like-charge attraction becomes apparently stronger when the particle charge is lower than a "critical" value, whereas such attraction gradually becomes weakened when the particle charge exceeds the "critical" value. Furthermore, our calculations indicate that the "critical" value decreases slightly with the increase of the salt concentration and decreases apparently for larger ions and larger charged colloidal particles. Finally, we derived an analytical formula for the "critical" particle charge based on the Lindemann melting law.

2. Results and Discussion. In this section, first, we calculate the PMFs between two like-charged colloidal particles with a wide range of particle charges in 2:2 and 3:3 salt solutions (see Figure 1), and the attractive PMFs mediated by multivalent ions exhibit a nonmonotonic dependence on the particle charge for both 2:2 and 3:3 salts around a "critical" particle charge. Afterward, we analyze the contributions of

electrostatic force and depletion force as well as counterion distributions to explore the microscopic mechanism for such nonmonotonic dependence on the particle charge. Additionally, we examine the effects of salt concentration, ion size, and colloidal particle size on the nonmonotonic dependence of multivalent ion-mediated like-charge attraction on the particle charge. Finally, we derive an analytical formula for the "critical" particle charge based on the Lindemann melting law.
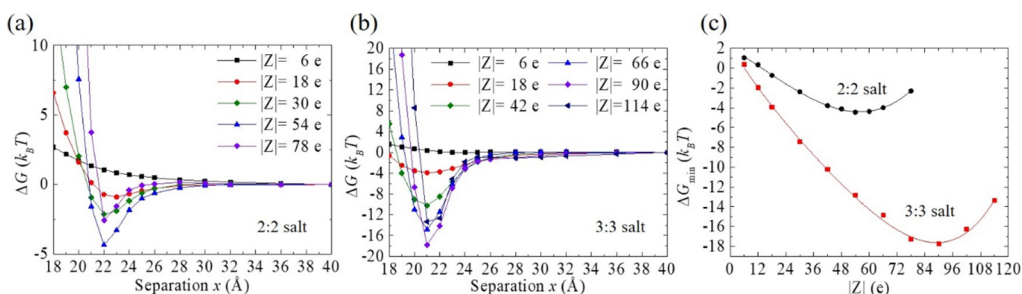
2.1. Effective Like-Charge Attraction is Nonmonotonically Dependent on the Particle Charge. As shown in Figure 2a,b, the PMFs between two like-charged colloidal particles are attractive and strongly dependent on the particle charge |Z| and the ion valence; see the complete PMFs for different |Z|'s in Figures S1a,b in the Supporting Information. For the 0.01 M 2:2 salt, as the particle charge |Z| is increased from 6 e to 54 e, the PMF changes gradually from a weak effective repulsion to a strong attraction, with the minimums of the PMFs at the separation of $x \sim 22$ Å. For a 0.1 mM 3:3 salt, the attractive PMF continuously becomes stronger when the particle charge |Z| is increased until |Z| ~ 90 e, with the minimums of the PMFs at the separation of $x \sim 21$ Å. Such an enhanced multivalent ion-mediated like-charge attraction by higher particle charges is in accordance with previous works.[52,54,83] The comparison between a 2:2 salt and a 3:3 salt indicates that trivalent counterions bind more tightly to charged colloidal particles and can cause a stronger effective attraction with a lower PMF minimum and a slightly closer equilibrium separation between like-charged colloidal particles.

It is also shown in Figure 2a,b that when the particle charge |Z| exceeds a high "critical" value |Z|$_c$, the PMFs between like-charged colloidal particles gradually become less attractive with the increase of |Z| for both 2:2 and 3:3 salts, which is beyond the prior expectation based on the results of low/medium particle charges and previous works.[34] To show such a phenomenon more directly, we utilized the minimum depth ΔG_{min} of the PMF to describe the strength of effective attractions between like-charged colloidal particles. As clearly shown in Figure 2c, with the increase of |Z|, negative ΔG_{min} decreases monotonically until a "critical" value and increases when |Z| exceeds the "critical" value. Namely, there is a nonmonotonic dependence of multivalent ion-mediated like-charge attraction on the particle charge for both 2:2 and 3:3 salts, and the "critical" values of particle charges are |Z|$_c \sim 54$ e for the 0.01 M 2:2 salt and |Z|$_c \sim 90$ e for the 0.1 mM 3:3 salt, respectively.

2.2. Driving Forces for Effective Like-Charge Attraction over a Wide Range of Colloidal Particle Charges. To understand the above-shown nonmonotonic dependence of the multivalent ion-mediated attraction between like-charged colloidal particles on particle charge, we first analyzed the driving forces for the effective like-charge attractions over a wide range of particle charges for 2:2 and 3:3 salts by calculating the electrostatic forces and depletion forces according to eqs 7 and 8; see Figures 3 and S2 in the Supporting Information. Afterward, we plot the minimum values of the electrostatic force and the depletion force (denoted F_{min}) versus the particle charge in Figure 3c,f, and the separations for the minimum value are chosen where the electrostatic forces and the depletion forces appear to be most attractive.

It is shown that there are roughly three regimes of colloidal particle charges associated with the electrostatic and depletion forces. At a low particle charge (up to |Z| ~ 18 e for the 2:2 salt

Figure 1. Schematic representation of the model system with two like-charged colloidal particles in a symmetrical multivalent (2:2 or 3:3) salt solution and x is the separation between the centers of the two colloidal particles. Here, the big spheres represent the colloidal particles with negative charge Z and the small spheres the salt ions.

Figure 2. (a,b) PMFs between like-charged colloidal particles in 0.01 M 2:2 (a) and 0.1 mM 3:3 (b) salt solutions from the MC simulations. (c) Dependence of the like-charge attraction strength on the colloidal particle charge in 0.01 M 2:2 salt (black) and 0.1 mM 3:3 salt (red) solutions. Lines in (c) are guide to the eye.
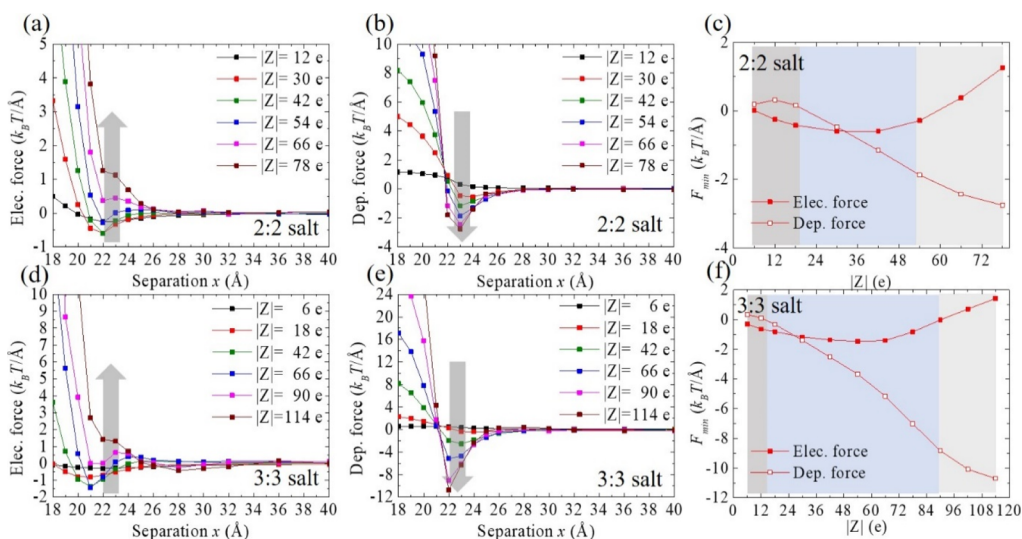

Figure 3. (a,b) Electrostatic forces between like-charged colloidal particles immersed in the 0.01 M 2:2 salt solution (a) and in the 0.1 mM 3:3 salt solution (b). (c,d) Depletion forces between like-charged colloidal particles immersed in the 0.01 M 2:2 salt solution (c) and in the 0.1 mM 3:3 salt solution (d). (e,f) Minimum values of the electrostatic force and depletion force over separation x versus the particle charge in the 0.01 M 2:2 salt solution (e) and in the 0.1 mM 3:3 salt solution (f). Full and open symbols represent the electrostatic force and the depletion force, respectively.

and up to $|Z| \sim 12$ e for the 3:3 salt), the electrostatic forces are obviously attractive and almost dominate the overall PMFs compared with the repulsive or weakly attractive depletion force. The effective like-charge attraction in this range of particle charge was attributed to the obviously attractive electrostatic force caused by the accumulation and bridging effect of counterions in the region between two like-charged colloidal particles.[13,84] As the particle charge rises up to $|Z| \sim 54$ e for the 2:2 salt and $|Z| \sim 90$ e for the 3:3 salt, the attractive electrostatic force between colloidal particles is not very sensitive to the particle charge and does not play a dominating role in determining the overall PMFs any longer compared to the strongly attractive depletion forces. The attractive depletion force is attributed to the Coulomb depletion and the resultant imbalance of counterions inside and outside the charged colloidal particles, which is a combined effect of the Coulomb attraction between colloidal particles and counterions and the strong Coulomb repulsion between condensed counterions.[52] As the particle charge exceeds $|Z| \sim 54$ e for the 2:2 salt and $|Z| \sim 90$ e for the 3:3 salt, the attractive electrostatic forces apparently increase to repulsive ones and become more repulsive for higher particle charges, while the depletion forces become slightly more attractive. Consequently, the attractive PMFs become weakened in this particle charge range; see Figure 3c,f.

Therefore, based on the above analyses, we can draw the following conclusions: (i) according to the components of driving forces, the like-charge attraction mediated by multivalent ions for a wide range of colloidal particle charges can be roughly divided into three particle-charge regimes, that is, the regime with an attractive electrostatic force and a repulsive/weakly attractive depletion force, that with an attractive electrostatic force and an attractive depletion force, and that with a repulsive electrostatic force and an attractive depletion force; (ii) the nonmonotonic dependence of multivalent ion-mediated like-charge attraction on the particle charge is mainly attributed to the transition of the electrostatic force from attraction to repulsion when the particle charge exceeds the "critical" value. The transition of electrostatic force from attraction to repulsion at a high particle charge is explicitly shown above and the mechanism will be discussed below.

2.3. Distribution of Ions around Colloidal Particles Is Responsible for Driving Forces. To understand the nonmonotonic dependence of multivalent ion-mediated like-charge attractions on the particle charge at the microscopic level, we analyzed the distribution of the counterions condensed on the surface of colloidal particles since the electrostatic and depletion forces are both determined by the condensed counterions around colloidal particles. As shown in the top portion of Figure 4a, the distribution of counterions
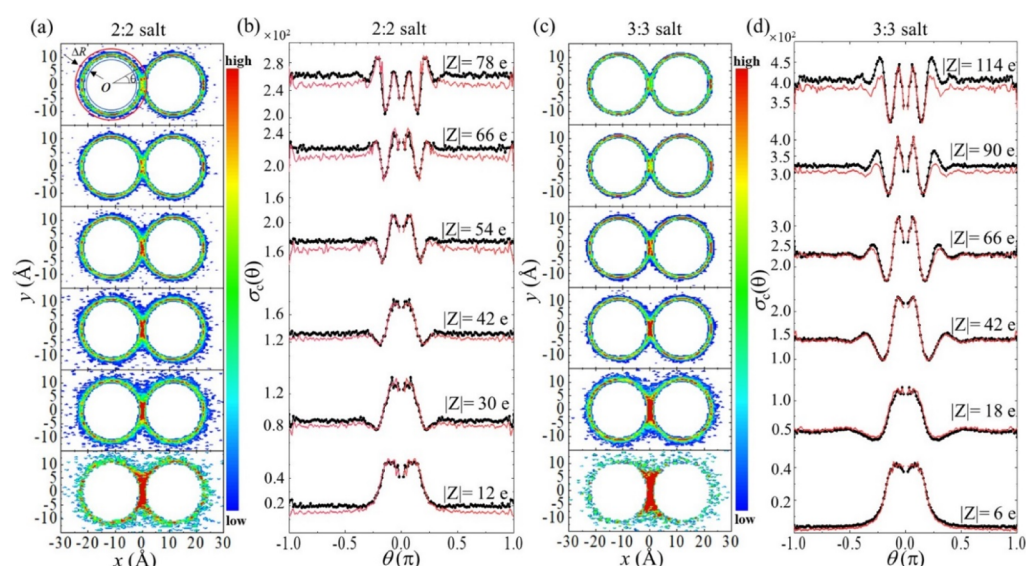
Figure 4. (a) Two-dimensional distribution of counterions around colloidal particles with different charges in the 0.01 M 2:2 salt solution. (b) Charge density $\sigma_c(\theta)$ of the condensed counterion around one colloidal particle with different charges in the 0.01 M 2:2 salt solution (black) and in the 0.1 mM 2:2 salt (red) solution. From bottom to top: $|Z| = 12$ e to $|Z| = 78$ e. (c) Two-dimensional distribution of counterions around colloidal particles with different charges in the 0.1 mM 3:3 salt solution (black) and in the 0.01 M 3:3 salt (red) solution. (d) Angular density $\sigma_c(\theta)$ of the condensed counterions around one colloidal particle with different charges in the 0.1 mM 3:3 salt solution. From bottom to top: $|Z| = 6$ e to $|Z| = 114$ e. Here, the particle−particle separation x was taken as a typical value $x = 2R + 2r_{ion} + 1$ Å for all panels; see the main text.

near the particle surface depends mainly on the polar angle θ with respect to the X-axis at close separation. Here, we used the charge density $\sigma_c(\theta)$ of condensed counterions within a condensation shell of a thickness of $\Delta R = r_{ion} + 2$ Å at the particle surface to analyze the electrostatic and depletion forces and the slight change of ΔR does not visibly affect our following analyses; see Figure S3 in the Supporting Information. Figure 4 shows the two-dimensional landscapes of counterion distributions and the charge densities $\sigma_c(\theta)$ of condensed counterions around two colloidal particles with different particle charges $|Z|$ for the 2:2 salt and at the 3:3 salt where the inter-particle separation was taken as a typical value of $x = 2R + 2r_{ion} + 1$ Å.

As shown in Figure 4, for low particle charges ($|Z| < \sim30$ e for the 2:2 salt and $|Z| < \sim18$ e for the 3:3 salt), there are apparently condensed bridging ions between two like-charged colloidal particles for both 2:2 and 3:3 salts, reflected by the high density of counterions and apparent peak in $\sigma_c(\theta)$ between two charged colloidal particles, that is, around $|\theta| \sim 0$. With the increase of the particle charge (up to ~54 e for the 2:2 salt and up to ~66 e for the 3:3 salt), the condensed bridging ions gradually becomes less apparent, and simultaneously the ion depletion zone begins to appear apparently, reflected by the relatively decreased peak height and the apparent valley depth in $\sigma_c(\theta)$ between two charged colloidal particles. When the particle charge becomes very high ($|Z| > 66$ e for the 2:2 salt and $|Z| > 90$ e for the 3:3 salt), the bridging ions nearly disappear and ion depletion becomes very apparent, as shown by the crystal-like charge density $\sigma_c(\theta)$ with almost a disappeared peak and a very apparent valley. The apparent crystal-like structure suggested that the Coulomb depletion can not only affect the depletion force but also affect the electrostatic force.

The electrostatic and depletion forces are strongly associated with the peak height of $\sigma_c(\theta)$ for bridging ions and the valley depth for ion depletion, respectively.[14] At a low particle charge, there is an apparent peak of bridging ions and no valley

(depletion zone), and correspondingly, the electrostatic force is attractive and the depletion force is repulsive. As the particle charge is increased, more bridging ions are necessary to be condensed to counteract the repulsion between like-charged colloidal particles to induce an effective like-charge attraction. However, for a very high particle charge, bridging ions cannot increase continuously and even decrease relatively to condensed counterions outside with the increase of the particle charge due to the Coulomb depletion (repulsion) between condensed counterions and the valley of $\sigma_c(\theta)$ in the limited region between two colloidal particles. Consequently, with the increase of the particle charge, the electrostatic force becomes more attractive for low particle charges while it can become repulsive at very high particle charges. Simultaneously, the depletion force is repulsive at a low particle charge $|Z|$ and become (more) attractive with the increase of $|Z|$ due to the more apparent valley of $\sigma_c(\theta)$ and the consequent stronger collisions from condensed counterions outside than those inside the two colloidal particles. It is also shown in Figure 4 that the more apparent peak height and valley depth of $\sigma_c(\theta)$ at high particle charges for the 0.1 mM 3:3 salt than that for the 0.01 M 2:2 salt suggests that the attractive electrostatic and depletion forces induced by trivalent counterions is generally stronger than those induced by divalent ones, and therefore the effective like-charge attractions for the 3:3 salt are generally stronger than those for the 2:2 salt.

To characterize the strength of Coulomb depletion, we introduce a reduced distance $d/2r_{ion}$ between neighboring condensed counterions relative to the diameter of the counterions. Here, d can be measured by the distance between the first peak and the second peak of the charge densities $\sigma_c(\theta)$ shown in Figure 4b,d, and a smaller $d/2r_{ion}$ corresponds to a stronger Coulomb depletion. As shown in Figure 5a,b, with the increase of particle charge $|Z|$, the reduced distance $d/2r_{ion}$ decreases and approaches ~1 at an extremely high particle charge, where $d/2r_{ion} \sim 1$ means the minimum distance between counterions before overlapping. This indicates that
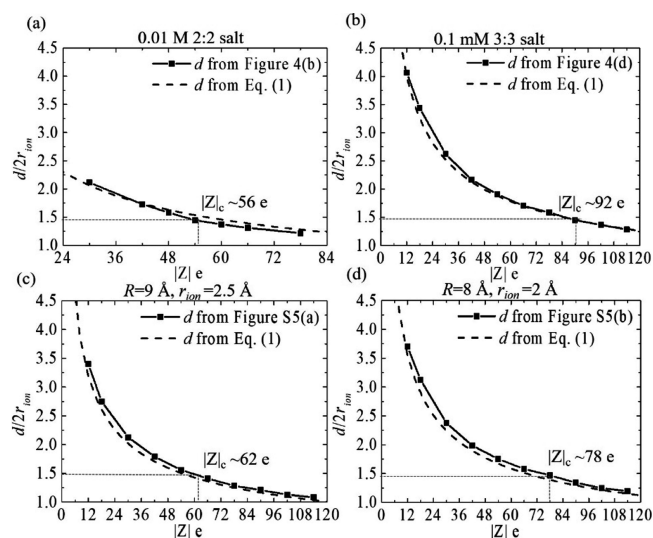
Figure 5. Reduced distance $d/2r_{\mathrm{ion}}$ between adjacent condensed counterions on the colloidal particle surface. (a) For the case of 0.01 M 2:2 salt, colloidal particle radii $R = 9$ Å and ion radii $r_{\mathrm{ion}} = 2$ Å; (b) For the case of 0.1 mM 3:3 salt, colloidal particle radii $R = 9$ Å and ion radii $r_{\mathrm{ion}} = 2$ Å; (c) For the case of 0.1 mM 3:3 salt, colloidal particle radii $R = 9$ Å and ion radii $r_{\mathrm{ion}} = 2.5$ Å; (d) For the case of 0.1 mM 3:3 salt, colloidal particle radii $R = 8$ Å and ion radii $r_{\mathrm{ion}} = 2$ Å. See also Figures 4 and S5a in the Supporting Information.

the strength of Coulomb depletion increases with the increase of the particle charge, that is, the crystal-like structure becomes more apparent at a higher particle charge. Interestingly, when the reduced distances $d/2r_{\mathrm{ion}}$ decrease to a value slightly smaller than 1.5, $|Z|$'s are close to the "critical" values $|Z|_c$ for both the 2:2 salt and the 3:3 salt though the "critical" particle charge $|Z|_c$ for the 2:2 salt is visibly lower than that for the 3:3 salt.

Based on the above analyses, we can understand the mechanism for the nonmonotonic colloidal particle-charge dependence of the like-charge attraction as follows. When the particle charge becomes very high, the counterion condensation in the limited region between two particles is suppressed severely due to the Coulomb depletion; thus, the attractive electrostatic force will become less attractive and even repulsive since the suppressed counterion condensation and bridging effect between two particles cannot compensate for the increased Coulomb repulsion between like-charged particles with higher charges. Consequently, the like-charge attraction dominated by the attractive depletion force becomes

weakened by the repulsive electrostatic force for a very high particle charge. Furthermore, we found that the "critical" particle charge $|Z|_c$ corresponds to the reduced distance between adjacent condensed counterions $d/2r_{\mathrm{ion}} \sim <1.5$ for both the 2:2 and 3:3 salts.

2.4. Salt Concentration Effect. To examine the effect of the salt concentration on the nonmonotonic dependence of the like-charge attraction between colloidal particles on particle charge, we made additional calculations of the PMFs for different 2:2 and 3:3 salt concentrations. As shown in Figure 6a,b, when the salt concentration decreases, the "critical" particle charge $|Z|_c$ increases slightly and the negative ΔG_{min} increases for both 2:2 and 3:3 salts. At a lower salt concentration, the less negative ΔG_{min} corresponds to the weaker effective like-charge attraction, which is attributed to the higher entropy penalty for counterion condensation and the resultant weaker counterion condensation.

In order to understand the higher "critical" particle charge $|Z|_c$ at a lower salt concentration, we calculated the charge density $\sigma_c(\theta)$ of condensed counterions around the colloidal particles since the suppression of counterion condensation in the limited region between two particles is mainly responsible for the appearance of the "critical" particle charge as discussed above. As shown in Figure 4b,d, a higher concentration leads to a lower relative peak height of bridging ions because there is no noticeable change of the ion condensation in the intervening region between two colloidal particles (i.e., region of $|\theta| < 0.15\pi$), while the counterion condensation in the outer region becomes slightly stronger. This suggests that the suppression of counterion condensation in the intervening region at a higher salt concentration is more severe due to the stronger Coulomb depletion, and consequently the electrostatic force begins to become repulsive at a lower $|Z|$ for the higher salt. Therefore, the "critical" particle charge $|Z|_c$ for the nonmonotonic dependence of effective like-charge attraction on the particle charge decreases slightly with the increase of the 2:2 or 3:3 salt concentration. However, such effect of 2:2 and 3:3 salt concentrations is still very slight, and this is because the multivalent ions can interact very strongly with charged colloidal particles and the condensation of multivalent ions is only weakly dependent on the salt concentration.[86]

2.5. Ion Size Effect. To examine the ion size effect for the dependence of the like-charge attraction between colloidal particles on particle charge, we made another series of calculations on the PMFs between two like-charged colloidal particles at the 0.1 mM 3:3 salt with larger ion radii ($r_{\mathrm{ion}} = 2.5$ Å). As shown in Figures 7a,b and S1 (c) in the Supporting Information, the PMFs for $r_{\mathrm{ion}} = 2.5$ Å are less attractive than
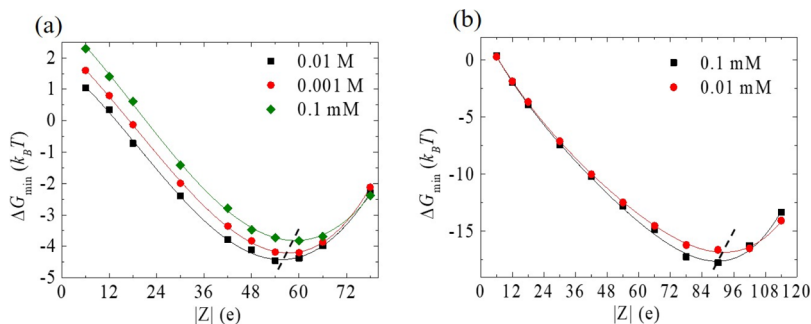
Figure 6. Nonmonotonic dependence of the like-charge attraction strength on the colloidal particle charge for the 2:2 salt solution (a) and for the 3:3 salt solution (b).
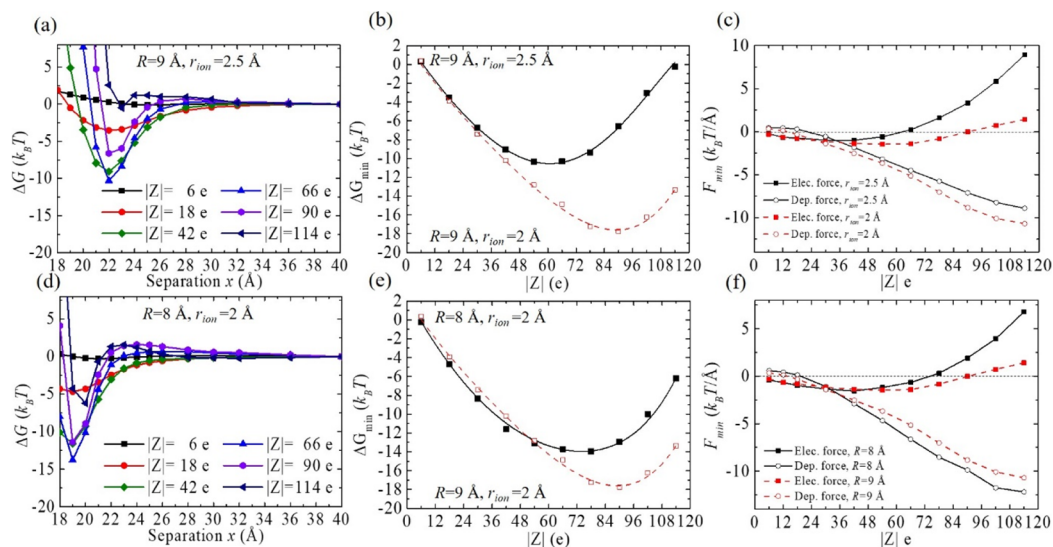
Figure 7. (a) PMFs between like-charged colloidal particles with radii $R = 9$ Å in the 0.1 mM 3:3 salt solution with radii $r_{ion} = 2.5$ Å from the MC simulations. (b) Dependence of the like-charge attraction strength on the particle charge in the 0.1 mM 3:3 salt solution: $R = 9$ Å and $r_{ion} = 2.5$ Å (black); $R = 9$ Å and $r_{ion} = 2$ Å (red). (c) Minimum values of the electrostatic force and the depletion force versus the particle charge in the 0.1 mM 3:3 salt solution: $R = 9$ Å and $r_{ion} = 2.5$ Å (black); $R = 9$ Å and $r_{ion} = 2$ Å (red). (d) PMFs between like-charged colloidal particles with radii $R = 8$ Å in the 0.1 mM 3:3 salt solution with radii $r_{ion} = 2$ Å from the MC simulations. (e) Dependence of the like-charge attraction strength on the particle charge in the 0.1 mM 3:3 salt solution: $R = 8$ Å and $r_{ion} = 2$ Å (black); $R = 9$ Å and $r_{ion} = 2$ Å (red). (f) Minimum values of the electrostatic force and depletion force over separation x versus the particle charge in the 0.1 mM 3:3 salt solution: $R = 8$ Å and $r_{ion} = 2$ Å (black); $R = 9$ Å and $r_{ion} = 2$ Å (red). Lines in (b,e) are guide to the eye.

for $r_{ion} = 2$ Å and the "critical" particle charge ($|Z|_c \sim 60$ e) for $r_{ion} = 2.5$ Å is apparently lower than that ($|Z|_c \sim 90$ e) for $r_{ion} = 2$ Å. To understand the ion size effect, we plot the minimum values of electrostatic force and depletion force as functions of particle charge $|Z|$ in Figures 7c and S4a−c in the Supporting Information. As shown in Figures 7 and S4a−c in the Supporting Information, the effective attraction weakening at a high charge is obviously attributed to the repulsive electrostatic force at a high particle charge, given that the attractive depletion force always becomes stronger with the increase of the particle charge. Furthermore, Figure 7c shows that the electrostatic force for $r_{ion} = 2.5$ Å becomes repulsive at a lower particle charge and is more repulsive than that for $r_{ion} = 2$ Å at a high particle charge, while the depletion force for $r_{ion} = 2.5$ Å is less attractive than that for $r_{ion} = 2$ Å at a high particle charge. Thus, compared with the case of $r_{ion} = 2$ Å, the PMFs for $r_{ion} = 2.5$ Å are less attractive and the enhanced trend of the attractive depletion force by a higher particle charge for $r_{ion} = 2.5$ Å could be counteracted by a repulsive electrostatic force at a lower particle charge and consequently, the effective like-charge attraction becomes weakened at a lower "critical" particle charge for larger ions.

Similar to the analyses in the above subsections, the disappearance of bridging ions due to the strong Coulomb depletion in the intervening space between two colloidal particles is responsible for the weakening of like-charge attraction at a high particle charge; see Figure S5a in the Supporting Information. It indicates that the Coulomb depletion for larger ions is stronger than that for the smaller ones, causing a lower "critical" particle charge $|Z|_c$ for the case of larger ions; see Figure 5c. It is worth noting that the reduced distance $d/2r_{ion}$ at the "critical" particle charge $|Z|_c$ for $r_{ion} = 2.5$ Å is also slightly smaller than ~1.5.

2.6. Effect of Particle Size. We have also made the calculations for smaller like-charged colloidal particles with $R =$

8 Å to examine the effect of particle size for the dependence of the like-charge attraction between colloidal particles on particle charge $|Z|$. As shown in Figures 7c,d and S1d in the Supporting Information, the multivalent ion-mediated attraction becomes weakened at a lower particle charge ($|Z|_c \sim 80$ e) compared with that for the charged colloidal particle with radii $R = 9$ Å ($|Z|_c \sim 90$ e). Such a lower $|Z|_c$ for smaller colloidal particles is attributed to the relations between the repulsive electrostatic force and the particle charge. As shown in Figures S4d−f in the Supporting Information, the electrostatic force at a high particle charge for $R = 8$ Å becomes repulsive at a lower particle charge and becomes rapidly more repulsive with $|Z|$ than that for $R = 9$ Å, while the depletion force for $R = 8$ Å is only slightly more attractive than that for $R = 9$ Å. Thus, the attractive depletion force for $R = 8$ Å can be counteracted by a strong repulsive electrostatic force at a lower $|Z|$, and consequently, the nonmonotonic dependence appears at a lower "critical" $|Z|_c$ for smaller charged colloidal particles.

Similar to the proceeding analyses, the disappearance of the bridging ions' peak in $\sigma_c(\theta)$ due to the strong Coulomb depletion in the intervening space between two colloidal particles is responsible for the weakening of like-charge attraction at a high particle charge; see Figure S5b in the Supporting Information. The more apparent Coulomb depletion for a smaller particle size is reasonable. First, counterions are more difficult to condense to serve as bridging ions in the more limited region between two smaller particles. Second, compared to larger colloidal particles, the smaller ones will attract more counterions to condense on the smaller surface area, and thus the average distance is reduced and the resultant Coulomb repulsion between condensed counterions enhanced. As shown in Figure 5b,d, the reduced distance $d/2r_{ion}$ between condensed counterions for the smaller particles is obviously smaller than that for the larger ones. This indicates that the Coulomb depletion for the smaller colloidal particle is
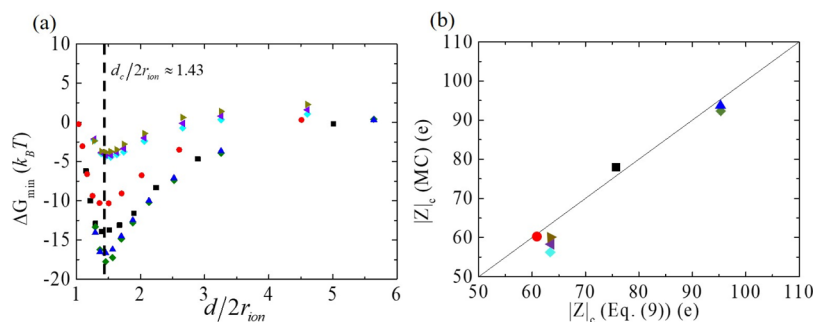
Figure 8. (a) Minimum values of the PMFs between like-charged colloidal particles as a function of the distance $d/2\,r_{ion}$ for system parameters; see eq 1 for d in the main text. (b) "Critical" particle charge $|Z|_c$ (MC) from the MC simulations versus $|Z|_c$ (eq 4) from eq 4. Due to the spare data in the MC simulations, $|Z|_c$ (MC) were obtained by the interpolation based on the MC data. Red symbols: 0.1 mM 3:3 salt, $R = 9$ Å and $r_{ion} = 2.5$ Å; black symbols: 0.1 mM 3:3 salt, $R = 8$ Å and $r_{ion} = 2$ Å; olive symbols: 0.1 mM 3:3 salt, $R = 9$ Å and $r_{ion} = 2$ Å; blue symbols: 0.01 mM 3:3 salt, $R = 9$ Å and $r_{ion} = 2$ Å; cyan symbols: 0.01 M 2:2 salt, $R = 9$ Å and $r_{ion} = 2$ Å; purple symbols: 0.001 M 2:2 salt, $R = 9$ Å and $r_{ion} = 2$ Å; brown symbols: 0.1 mM 2:2 salt, $R = 9$ Å and $r_{ion} = 2$ Å.

stronger than that for the larger ones, which causes a more repulsive electrostatic force and a lower "critical" particle charge $|Z|_c$ for the smaller colloidal particles. Furthermore, we found that the reduced distance $d/2r_{ion}$ at $|Z|_c$ for $R = 8$ Å and $r_{ion} = 2$ Å is close to a value slightly smaller than 1.5, which is consistant with the above discussed cases.

2.7. Analytical Formula for the "Critical" Particle Charge. Based on the above extensive MC simulations and analyses, the nonmonotonic dependence of like-charge attraction between colloidal particles on the particle charge is attributed to the Coulomb depletion of condensed counterions at a high particle charge, which suppresses the counterion condensation in the intervening space between two like-charged colloidal particles. In the following, we will derive an analytical formula for the "critical" particle charge. As shown above, the distance d between two adjacent condensed counterions can be used to measure the strength of Coulomb depletion of condensed counterions, and d is given by[63,87]

$$d = 2R\sqrt{\left|\frac{q}{Z}\right|\pi} \tag{1}$$

where q is the charge of the counterions. d is derived based on the assumption that the charged colloidal particles were fully neutralized[63,87,88] and such an assumption is obviously valid for our multivalent ion-particle systems; see Figure S3 in the Supporting Information. As shown in Figure 5, d from eq 1 agrees well with the values from the MC simulations. Inspired by the formation of the crystal-like structure of condensed counterions around the "critical" particle charge $|Z|_c$ and following previous works,[88−90] we used the Lindemann melting law to characterize the strong Coulomb depletion of condensed counterions at $|Z|_c$. Thus, the distance between adjacent condensed counterions d_c at the "critical" $|Z|_c$ satisfies

$$d_c \approx 2(r_{ion} + \Delta r) \tag{2}$$

where Δr is the fluctuation displacement of condensed counterions around its equilibrium position. Here, $d > d_c$ and $d < d_c$ correspond to the liquid-like state and crystal-like state of condensed counterions, respectively. According to the Lindemann melting law, $\Delta r = 0.15d_c$ corresponds to the value of the solid−liquid transition.[86,88] Then, eq 2 gives

$$\frac{d_c}{2r_{ion}} \approx 1.43 \tag{3}$$

As shown in Figure 8a, eq 3 agrees well with the extensive MC simulations over system parameters including ion valence, ion size, ion concentration, and colloidal particle size. Furthermore, the combination of eqs 1 and 3 gives the "critical" particle charge $|Z|_c$

$$|Z|_c = \frac{|q|\pi R^2}{2r_{ion}^2} \tag{4}$$

As shown in Figure 8b, $|Z|_c$'s from eq 4 are nearly in quantitative accordance with those from the MC simulations including system parameters.

Therefore, we can generalize the weakening of multivalent ion-mediated attraction between two like-charged colloidal particles at a high particle charge as follows: when particle charge $|Z|$ becomes very high and exceeds the "critical" value $|Z|_c$, the condensed counterions transit from the liquid state to the crystal one due to the very strong Coulomb depletion. This would lead to the repulsive electrostatic force, which counteracts the attractive depletion force and consequently results in the effective attraction weakening. If the condensed counterions are modeled as one component plasma,[1] such weakening of multivalent ion-mediated attraction would correspond to the phase transition from the liquid state to the crystal one for one component plasma.

3. CONCLUSIONS

In summary, in the present work, we made extensive Monte Carlo simulations for calculating the PMF between like-charged colloidal particles with a wide range of particle charges for both divalent and trivalent salts of different concentrations. Through extensive calculations and detailed analyses, we have reached the following major conclusions:

(1) The multivalent ion-mediated attraction between like-charged colloidal particles is nonmonotonically dependent on particle charge: with the increase of particle charge, the effective attraction is apparently strengthened when the particle charge is lower than a "critical" value, while such attraction would become gradually weakened when the particle charge exceeds the "critical" value. The "critical" particle charge for the 3:3 salt is higher than that for the 2:2 salt.

(2) The driving forces for effective attraction between like-charged colloidal particles mediated by divalent/trivalent ions could be divided into three particle-charge regimes:

(i) a low particle charge regime with an attractive electrostatic force and a repulsive/weakly attractive depletion force; (ii) a medium particle charge regime with an attractive electrostatic force and an attractive depletion force; (iii) a high particle charge regime with a repulsive electrostatic force and an attractive depletion force.

(3) The nonmonotonic dependence of the multivalent ion-mediated like-charge attraction on particle charge is attributed to the unexpected repulsive electrostatic force induced by Coulomb depletion, which suppresses the counterion condensation in the limited region between colloidal particles.

(4) The "critical" particle charge decreases apparently for larger ions and smaller colloidal particles due to the stronger Coulomb depletion effects for larger ions and smaller colloidal particles and decreases slightly at a higher salt concentration due to the slightly enhanced Coulomb depletion of counterions between colloidal particles.

(5) We derived an analytical formula for the "critical" particle charge based on the Lindemann melting law and such a formula agrees well with our extensive MC simulations including system parameters.

In spite of the above major conclusions, our model system involves some important simplifications. First, the charges of colloidal particles were placed at the centers of the respective particles and consequently the discreteness of the particle charges at the surfaces was ignored. Such simplification may affect counterion distributions in the very close vicinity of colloidal particles. Second, the solvent was modeled as a continuous dielectric medium, and the dielectric boundary between particles and solvent was ignored. In fact, colloidal particles generally have a lower dielectric constant than the solvent outside,[91−93] and counterions at the particle surface would experience the repulsion from the induced ion image charges, which would disfavor the counterion condensation.[93−95] Such an effect may be partially compensated by the enhanced electrostatic attraction between counterions and particles with a low dielectric constant.[86] Third, for simplicity, divalent and trivalent salts were modeled as symmetrical 2:2 and 3:3 salts with equal ion sizes rather than realistic salts. Although these simplifications were often used in previous model systems for ion−particle interactions, more detailed and accurate treatments are still required to be involved in future works, including discrete charge distributions, a discontinuous dielectric boundary effect, and more realistic (mixed) salts. Nevertheless, our finding and analyses can be very helpful for understanding the ion-mediated effective interactions between charged colloidal particles and the assembly of charged colloidal particles.

4. MODEL AND METHOD

In this work, we investigated effective interactions between like-charged colloidal particles in symmetrical multivalent salt solutions by canonical ensemble MC simulations based on a primitive model in which salt ions were considered as small charged spheres and the solvent was modeled as a continuum medium with a dielectric constant ε.[54] In our simulations, two large like-charged colloidal particles were immersed in a rectangular box and the particles were symmetrically located on two sides of the plane at $x = 0$. For simplicity, interactions between charged colloidal particles and ions are composed of Coulombic interactions and hard-core interactions

$$u_{ij} = \begin{cases} \dfrac{q_i q_j}{4\pi\varepsilon_0\varepsilon r_{ij}} & r_{ij} \geq a_i + a_j \\ \infty & r_{ij} \leq a_i + a_j \end{cases} \qquad (5)$$

here, a_i and q_i stand for the radius and charge of sphere i (small ions and large colloidal particles), and r_{ij} is the center-to-center distance between spheres i and j. ε_0 and ε are the vacuum permittivity and the dielectric constant of the solvent, respectively. In practice, to diminish the boundary effect, the sizes of simulation boxes were always kept larger than two colloidal particles by at least 6 times the Debye−Hückel length, and the calculated results are stable as tested against different box sizes. In the model system, we fixed the radii of two colloidal particles R to 9 Å, the radii of salt ions r_{ion} to 2 Å, and the temperature to 298.15 K (room temperature) in all the MC simulations. Our simulation systems are illustrated in Figure 1. The charge Z of colloidal particles ranges from −6 to −78 e for the 2:2 salt and ranges from −6 to −114 e for the 3:3 salt, respectively. Furthermore, we made the calculations for a different colloidal particle size (R = 8 Å) and a different ion size (r_{ion} = 2.5 Å) to examine the colloidal particle size effect and ion size effect. Additionally, we made the calculations for different concentrations of the 2:2 salt and the 3:3 salt to examine the salt concentration effect.

In our simulations, the Metropolis algorithm[96] was employed to generate the distributions of ions at equilibrium. Each MC simulation starts from an initial configuration with fixed colloidal particles in the X-axis with separation x and randomly distributed ions, and the probability to accept a trial move of an ion is given by $p = \min[1,\exp(-\Delta U/k_BT)]$, where ΔU is the interaction energy change associated with the trial move of the ion in the simulation box. k_B is the Boltzmann constant, and T is the absolute temperature in Kelvin. Six million configurations were collected to calculate the average mean force after the pre-equilibrium process.

The total mean force acting on colloidal particle i along the reaction coordinate (the X-axis) is composed of two terms

$$F_{total}{}^i(x) = F_{ele}{}^i(x) + F_{hs}{}^i(x) \qquad (6)$$

Here, $F_{ele}^i(x)$ is the electrostatic force between colloidal particle i and all other charged objects, and $F_{hs}^i(x)$ is the depletion force (hard-sphere collision force) between colloidal particle i and the counterions in contact with it. The electrostatic force $F_{ele}^i(x)$ is expressed as[40,52,54,97]

$$F_{ele}^i(x) = -\left\langle \sum_{j\neq i} \frac{\partial u_{ij}}{\partial x} \right\rangle$$

$$= \frac{z_i^2}{4\pi\varepsilon_0\varepsilon x^2} + \left\langle \sum_{j\neq i} \frac{Z_i q_j}{4\pi\varepsilon_0\varepsilon r_{ij}^2}\cos(\theta) \right\rangle \qquad (7)$$

where θ is the polar angle formed with the reaction coordinate and the angular brackets···denote the ensemble average. x is the separation between two colloidal particles and r_{ij} is the distance between colloidal particle i and ion j. Z_i and q_j are charges of colloidal particle i and ion j, respectively. The depletion force $F_{hs}^i(x)$ based on the contact theorem in spherical geometry is given by

$$F_{hs}{}^{i}(x) = -k_{B}T \left\langle \sum_{\theta=-\pi}^{\pi} \frac{n(\theta)}{\Delta R} \cos(\theta) \right\rangle \tag{8}$$

where $n(\theta)$ is the number of counterions located in a spherical shell with polar angle θ and thin thickness ΔR at the surface of colloidal particle i. In practice, $\Delta R = 0.02$ Å was used in our calculations for the calculation accuracy and efficiency and the choice of ΔR around the value does not have a visible influence on our calculated results. The PMFs were calculated through integrating the ensemble-averaged mean forces along the reaction coordination x to describe the effective interactions between like-charged colloidal particles in multivalent salt solutions.[40,52,54,97] Thus, the PMF $\Delta G(x)$ can be calculated numerically as[40,54]

$$\Delta G(x) = -\int_{x_{ref}}^{x} F_{total}{}^{i}(x)dx \tag{9}$$

where the outer reference separation was taken as $x_{ref} = 40$ Å in practice.

■ ASSOCIATED CONTENT

Ⓢ Supporting Information

The Supporting Information is available free of charge at https://pubs.acs.org/doi/10.1021/acsomega.1c00613.

> PMFs between like-charged colloidal particles with a wide range of particle charges in 2:2 and 3:3 salt solutions; electrostatic forces and the depletion forces between like-charged colloidal particles in 2:2 and 3:3 salt solutions; definition of the charge fraction of the counterions condensed on the surface of colloidal particles; and condensed charge density $\sigma_c(\theta)$ of counterions under different conditions for different particle charges |Z| (PDF)

■ AUTHOR INFORMATION

Corresponding Authors

Jie Huo − *Center for Theoretical Physics and Key Laboratory of Artificial Micro & Nano-structures of Ministry of Education, School of Physics and Technology, Wuhan University, Wuhan 430072, China; School of Physics and Electronic-Electrical Engineering, Ningxia University, Yinchuan 750021, China;* Email: huojie@nxu.edu.cn

Zhi-Jie Tan − *Center for Theoretical Physics and Key Laboratory of Artificial Micro & Nano-structures of Ministry of Education, School of Physics and Technology, Wuhan University, Wuhan 430072, China;* ⓘ orcid.org/0000-0002-7367-0182; Email: zjtan@whu.edu.cn

Authors

Cheng Lin − *Center for Theoretical Physics and Key Laboratory of Artificial Micro & Nano-structures of Ministry of Education, School of Physics and Technology, Wuhan University, Wuhan 430072, China*

Xiaowei Qiang − *Center for Theoretical Physics and Key Laboratory of Artificial Micro & Nano-structures of Ministry of Education, School of Physics and Technology, Wuhan University, Wuhan 430072, China*

Hai-Long Dong − *Center for Theoretical Physics and Key Laboratory of Artificial Micro & Nano-structures of Ministry of Education, School of Physics and Technology, Wuhan University, Wuhan 430072, China*

Complete contact information is available at:
https://pubs.acs.org/10.1021/acsomega.1c00613

Notes
The authors declare no competing financial interest.

■ REFERENCES

(1) Levin, Y. Electrostatic Correlations: From Plasma to Biology. *Rep. Prog. Phys.* **2002**, *65*, 1577−1632.

(2) Chen, S.-J. Rna Folding: Conformational Statistics, Folding Kinetics, and Ion Electrostatics. *Annu. Rev. Biophys.* **2008**, *37*, 197−214.

(3) Pollack, L. Saxs Studies of Ion−Nucleic Acid Interactions. *Annu. Rev. Biophys.* **2010**, *40*, 225−242.

(4) Lipfert, J.; Doniach, S.; Das, R.; Herschlag, D. Understanding Nucleic Acid−Ion Interactions. *Annu. Rev. Biochem.* **2014**, *83*, 813−841.

(5) Knipe, P. C.; Thompson, S.; Hamilton, A. D. Ion-Mediated Conformational Switches. *Chem. Sci.* **2015**, *6*, 1630−1639.

(6) Hamilton, G. C. L.; Pollack, L. Electrostatics of Strongly Charged Biological Polymers: Ion-Mediated Interactions and Self-Organization in Nucleic Acids and Proteins. *Annu. Rev. Phys. Chem.* **2010**, *61*, 171−189.

(7) Sun, L.-Z.; Zhang, D.; Chen, S.-J. Theory and Modeling of Rna Structure and Interactions with Metal Ions and Small Molecules. *Annu. Rev. Biophys.* **2017**, *46*, 227−246.

(8) Fenley, M. O.; Russo, C.; Manning, G. S. Theoretical Assessment of the Oligolysine Model for Ionic Interactions in Protein-DNA Complexes. *J. Phys. Chem. B* **2011**, *115*, 9864−9872.

(9) Tian, W.-d.; Ma, Y.-q. Effects of Valences of Salt Ions at Various Concentrations on Charged Dendrimers. *Soft Matter* **2010**, *6*, 1308−1316.

(10) Xi, K.; Wang, F.-H.; Xiong, G.; Zhang, Z.-L.; Tan, Z.-J. Competitive Binding of Mg2+ and Na+ Ions to Nucleic Acids: From Helices to Tertiary Structures. *Biophys. J.* **2018**, *114*, 1776−1790.

(11) Tan, Z.-J.; Chen, S.-J. Ion-Mediated Rna Structural Collapse: Effect of Spatial Confinement. *Biophys. J.* **2012**, *103*, 827−836.

(12) Allahyarov, E.; Löwen, H. Effective Interaction between Helical Biomolecules. *Phys. Rev. E* **2000**, *62*, 5542−5556.

(13) Wu, J. Z.; Bratko, D.; Blanch, H. W.; Prausnitz, J. M. Interaction between Oppositely Charged Micelles or Globular Proteins. *Phys. Rev. E* **2000**, *62*, 5273−5280.

(14) Tan, Z.-J.; Chen, S.-J. Ion-Mediated Nucleic Acid Helix-Helix Interactions. *Biophys. J.* **2006**, *91*, 518−536.

(15) Jho, Y. S.; Brewster, R.; Safran, S. A.; Pincus, P. A. Long-Range Interaction between Heterogeneously Charged Membranes. *Langmuir* **2011**, *27*, 4439−4446.

(16) Qiu, X.; Khripin, C. Y.; Ke, F.; Howell, S. C.; Zheng, M. Electrostatically Driven Interactions between Hybrid DNA-Carbon Nanotubes. *Phys. Rev. Lett.* **2013**, *111*, 048301.

(17) Wu, Y.-Y.; Zhang, Z.-L.; Zhang, J.-S.; Zhu, X.-L.; Tan, Z.-J. Multivalent Ion-Mediated Nucleic Acid Helix-Helix Interactions: Rna Versus DNA. *Nucleic Acids Res.* **2015**, *43*, 6156−6165.

(18) Antila, H. S.; Van Tassel, P. R.; Sammalkorpi, M. Interaction Modes between Asymmetrically and Oppositely Charged Rods. *Phys. Rev. E* **2016**, *93*, 022602.

(19) Kanduč, M.; Moazzami-Gudarzi, M.; Valmacco, V.; Podgornik, R.; Trefalt, G. Interactions between Charged Particles with Bathing

Multivalent Counterions: Experiments Vs. Dressed Ion Theory. *Phys. Chem. Chem. Phys.* **2017**, *19*, 10069−10080.

(20) Zhang, Z.-L.; Wu, Y.-Y.; Xi, K.; Sang, J.-P.; Tan, Z.-J. Divalent Ion-Mediated DNA-DNA Interactions: A Comparative Study of Triplex and Duplex. *Biophys. J.* **2017**, *113*, 517−528.

(21) Moazzami-Gudarzi, M.; Adam, P.; Smith, A. M.; Trefalt, G.; Szilágyi, I.; Maroni, P.; Borkovec, M. Interactions between Similar and Dissimilar Charged Interfaces in the Presence of Multivalent Anions. *Phys. Chem. Chem. Phys.* **2018**, *20*, 9436−9448.

(22) Katz, A. M.; Tolokh, I. S.; Pabit, S. A.; Baker, N.; Onufriev, A. V.; Pollack, L. Spermine Condenses DNA, but Not Rna Duplexes. *Biophys. J.* **2017**, *112*, 22−30.

(23) Zhang, C.; Jin, G.; Ma, Y. -q. Effective Potential between Two Spheres in a Suspension of Adhesive Rods. *Phys. Rev. E* **2007**, *75*, 041406.

(24) Kumar, S.; Aswal, V. K.; Kohlbrecher, J. Small-Angle Neutron Scattering Study of Interplay of Attractive and Repulsive Interactions in Nanoparticle-Polymer System. *Langmuir* **2016**, *32*, 1450−1459.

(25) Zhao, K.; Mason, T. G. Assembly of Colloidal Particles in Solution. *Rep. Prog. Phys.* **2018**, *81*, 126601.

(26) Carnie, S. L.; Chan, D. Y. C.; Stankovich, J. Computation of Forces between Spherical Colloidal Particles: Nonlinear Poisson-Boltzmann Theory. *J. Colloid Interface Sci.* **1994**, *165*, 116−128.

(27) Pericet-Camara, R.; Papastavrou, G.; Behrens, S. H.; Borkovec, M. Interaction between Charged Surfaces on the Poisson−Boltzmann Level: The Constant Regulation Approximation. *J. Phys. Chem. B* **2004**, *108*, 19467−19475.

(28) Sharp, K. A.; Honig, B. Calculating Total Electrostatic Energies with the Nonlinear Poisson-Boltzmann Equation. *J. Phys. Chem.* **1990**, *94*, 7684−7692.

(29) Sens, P.; Joanny, J.-F. Counterion Release and Electrostatic Adsorption. *Phys. Rev. Lett.* **2000**, *84*, 4862−4865.

(30) Grosberg, A. Y.; Nguyen, T. T.; Shklovskii, B. I. Colloquium: The Physics of Charge Inversion in Chemical and Biological Systems. *Rev. Mod. Phys.* **2002**, *74*, 329−345.

(31) Besteman, K.; Zevenbergen, M. A. G.; Heering, H. A.; Lemay, S. G. Direct Observation of Charge Inversion by Multivalent Ions as a Universal Electrostatic Phenomenon. *Phys. Rev. Lett.* **2004**, *93*, 170802.

(32) Wen, Q.; Tang, J. X. Absence of Charge Inversion on Rodlike Polyelectrolytes with Excess Divalent Counterions. *J. Chem. Phys.* **2004**, *121*, 12666−12670.

(33) Skinner, B.; Shklovskii, B. I. Non-Monotonic Swelling of a Macroion Due to Correlation-Induced Charge Inversion. *Physica A* **2009**, *388*, 1−8.

(34) Zhang, J.-S.; Zhang, X.; Zhang, Z.-L.; Tan, Z. J. Potential of Mean Force between Oppositely Charged Nanoparticles: A Comprehensive Comparison between Poisson−Boltzmann Theory and Monte Carlo Simulations. *Sci. Rep.* **2017**, *7*, 14145.

(35) Su, M.; Xu, Z.; Wang, Y. Poisson−Boltzmann Theory with Non-Linear Ion Correlations. *J. Phys.: Condens. Matter* **2019**, *31*, 355101.

(36) Chen, D.; Chen, Z.; Chen, C.; Geng, W.; Wei, G.-W. Mibpb: A Software Package for Electrostatic Analysis. *J. Comput. Chem.* **2011**, *32*, 756−770.

(37) Su, M.; Wang, Y. A brief review of continuous models for ionic solutions: the Poisson-Boltzmann and related theories. *Commun. Theor. Phys.* **2020**, *72*, 067601.

(38) Lindgren, E. B.; Chan, H.-K.; Stace, A. J.; Besley, E. Progress in the Theory of Electrostatic Interactions between Charged Particles. *Phys. Chem. Chem. Phys.* **2016**, *18*, 5883−5895.

(39) Trulsson, M.; Jönsson, B.; Åkesson, T.; Forsman, J.; Labbez, C. Repulsion between Oppositely Charged Surfaces in Multivalent Electrolytes. *Phys. Rev. Lett.* **2006**, *97*, 068302.

(40) Antila, H. S.; Van Tassel, P. R.; Sammalkorpi, M. Repulsion between Oppositely Charged Rod-Shaped Macromolecules: Role of Overcharging and Ionic Confinement. *J. Chem. Phys.* **2017**, *147*, 124901.

(41) Lin, C.; Zhang, X.; Qiang, X.; Zhang, J.-S.; Tan, Z.-J. Apparent Repulsion between Equally and Oppositely Charged Spherical Polyelectrolytes in Symmetrical Salt Solutions. *J. Chem. Phys.* **2019**, *151*, 114902.

(42) Nguyen, T. T.; Rouzina, I.; Shklovskii, B. I. Reentrant Condensation of DNA Induced by Multivalent Counterions. *J. Chem. Phys.* **2000**, *112*, 2562−2568.

(43) Dai, L.; Mu, Y.; Nordenskiöld, L.; van der Maarel, J. R. Molecular Dynamics Simulation of Multivalent-Ion Mediated Attraction between DNA Molecules. *Phys. Rev. Lett.* **2008**, *100*, 118301.

(44) Drozdetski, A. V.; Tolokh, I. S.; Pollack, L.; Baker, N.; Onufriev, A. V. Opposing Effects of Multivalent Ions on the Flexibility of DNA and Rna. *Phys. Rev. Lett.* **2016**, *117*, 028101.

(45) Qiu, X.; Andresen, K.; Kwok, L. W.; Lamb, J. S.; Park, H. Y.; Pollack, L. Inter-DNA Attraction Mediated by Divalent Counterions. *Phys. Rev. Lett.* **2007**, *99*, 038104.

(46) Qiu, X.; Parsegian, V. A.; Rau, D. C. Divalent Counterion-Induced Condensation of Triple-Strand DNA. *Proc. Natl. Acad. Sci. U.S.A.* **2010**, *107*, 21482−21486.

(47) Srivastava, A.; Timsina, R.; Heo, S.; Dewage, S. W.; Kirmizialtin, S.; Qiu, X. Structure-Guided DNA-DNA Attraction Mediated by Divalent Cations. *Nucleic Acids Res.* **2020**, *48*, 7018−7026.

(48) Lau, A. W. C.; Pincus, P. Counterion Condensation and Fluctuation-Induced Attraction. *Phys. Rev. E* **2002**, *66*, 041501.

(49) Butler, J. C.; Angelini, T.; Tang, J. X.; Wong, G. C. L. Ion Multivalence and Like-Charge Polyelectrolyte Attraction. *Phys. Rev. Lett.* **2003**, *91*, 028301.

(50) Ray, J.; Manning, G. S. An Attractive Force between Two Rodlike Polyions Mediated by the Sharing of Condensed Counterions. *Langmuir* **1994**, *10*, 2450−2461.

(51) Ha, B.-Y.; Liu, A. J. Counterion-Mediated Attraction between Two Like-Charged Rods. *Phys. Rev. Lett.* **1997**, *79*, 1289−1292.

(52) Allahyarov, E.; D'Amico, I.; Löwen, H. Attraction between Like-Charged Macroions by Coulomb Depletion. *Phys. Rev. Lett.* **1998**, *81*, 1334−1337.

(53) Lyubartsev, A. P.; Tang, J. X.; Janmey, P. A.; Nordenskiöld, L. Electrostatically Induced Polyelectrolyte Association of Rodlike Virus Particles. *Phys. Rev. Lett.* **1998**, *81*, 5465−5468.

(54) Wu, J.; Bratko, D.; Prausnitz, J. M. Interaction between Like-Charged Colloidal Spheres in Electrolyte Solutions. *Proc. Natl. Acad. Sci. U.S.A.* **1998**, *95*, 15169−15172.

(55) Messina, R.; Holm, C.; Kremer, K. Strong Attraction between Charged Spheres Due to Metastable Ionized States. *Phys. Rev. Lett.* **2000**, *85*, 872−875.

(56) Kim, Y. W.; Yi, J.; Pincus, P. A. Attractions between Like-Charged Surfaces with Dumbbell-Shaped Counterions. *Phys. Rev. Lett.* **2008**, *101*, 208305.

(57) Moazzami-Gudarzi, M.; Kremer, T.; Valmacco, V.; Maroni, P.; Borkovec, M.; Trefalt, G. Interplay between Depletion and Double-Layer Forces Acting between Charged Particles in Solutions of Like-Charged Polyelectrolytes. *Phys. Rev. Lett.* **2016**, *117*, 088001.

(58) Tang, J. X.; Wong, S.; Tran, P. T.; Janmey, P. A. Counterion Induced Bundle Formation of Rodlike Polyelectrolytes. *Ber. Bunsen-Ges. Phys. Chem.* **1996**, *100*, 796−806.

(59) Dunstan, D. E. Forces between Mica Surfaces in Calcium Chloride Solutions. *Langmuir* **1992**, *8*, 740−743.

(60) Tata, B. V. R.; Mohanty, P. S.; Valsakumar, M. C. Bound Pairs: Direct Evidence for Long-Range Attraction between Like-Charged Colloids. *Solid State Commun.* **2008**, *147*, 360−365.

(61) Nagornyak, E.; Yoo, H.; Pollack, G. H. Mechanism of Attraction between Like-Charged Particles in Aqueous Solution. *Soft Matter* **2009**, *5*, 3850−3857.

(62) Oncsik, T.; Trefalt, G.; Csendes, Z.; Szilagyi, I.; Borkovec, M. Aggregation of Negatively Charged Colloidal Particles in the Presence of Multivalent Cations. *Langmuir* **2014**, *30*, 733−741.

(63) Wu, J.; Prausnitz, J. M. Generalizations for the Potential of Mean Force between Two Isolated Colloidal Particles from Monte Carlo Simulations. *J. Colloid Interface Sci.* **2002**, *252*, 326−330.

(64) Zheng, Y.; Lin, C.; Zhang, J. S.; Tan, Z. J. Ion-Mediated Interactions between Like-Charged Polyelectrolytes with Bending Flexibility. *Sci. Rep.* **2020**, *10*, 21586.

(65) Kirkwood, J. G.; Shumaker, J. B. Forces between Protein Molecules in Solution Arising from Fluctuations in Proton Charge and Configuration. *Proc. Natl. Acad. Sci. U.S.A.* **1952**, *38*, 863−871.

(66) Guldbrand, L.; Jönsson, B.; Wennerström, H.; Linse, P. Electrical Double Layer Forces. A Monte Carlo Study. *J. Chem. Phys.* **1984**, *80*, 2221−2228.

(67) Levin, Y. When Do Like Charges Attract? *Physica A* **1999**, *265*, 432−439.

(68) Oosawa, F. Interaction between Parallel Rodlike Macroions. *Biopolymers* **1968**, *6*, 1633−1647.

(69) Ma, N.; Girvin, S. M.; Rajaraman, R. Effective Attraction between Like-Charged Colloids in a Two-Dimensional Plasma. *Phys. Rev. E* **2001**, *63*, 021402.

(70) Stelmakh, A.; Cai, W.; Baumketner, A. Attraction between Like-Charged Macroions Mediated by Specific Counterion Configurations. *J. Phys. Chem. B* **2019**, *123*, 9971−9983.

(71) Li, Y.; Girard, M.; Shen, M.; Millan, J. A.; Olvera de la Cruz, M. Strong Attractions and Repulsions Mediated by Monovalent Salts. *Proc. Natl. Acad. Sci. U.S.A.* **2017**, *114*, 11838−11843.

(72) Paillusson, F.; Dahirel, V.; Jardat, M.; Victor, J.-M.; Barbi, M. Effective Interaction between Charged Nanoparticles and DNA. *Phys. Chem. Chem. Phys.* **2011**, *13*, 12603−12613.

(73) Trefalt, G.; Palberg, T.; Borkovec, M. Forces between Colloidal Particles in Aqueous Solutions Containing Monovalent and Multivalent Ions. *Curr. Opin. Colloid Interface Sci.* **2017**, *27*, 9−17.

(74) Besteman, K.; Zevenbergen, M. A. G.; Lemay, S. Charge Inversion by Multivalent Ions: Dependence on Dielectric Constant and Surface-Charge Density. *Phys. Rev. E* **2005**, *72*, 061501.

(75) Jho, Y. S.; Kanduč, M.; Naji, A.; Podgornik, R.; Kim, M.-W.; Pincus, P. A. Strong-Coupling Electrostatics in the Presence of Dielectric Inhomogeneities. *Phys. Rev. Lett.* **2008**, *101*, 188101.

(76) Wen, Q.; Tang, J. X. Temperature Effects on Threshold Counterion Concentration to Induce Aggregation of Fd Virus. *Phys. Rev. Lett.* **2006**, *97*, 048101.

(77) Nguyen, T. T. Grand-Canonical Simulation of DNA Condensation with Two Salts, Effect of Divalent Counterion Size. *J. Chem. Phys.* **2016**, *144*, 065102.

(78) Zelko, J.; Iglič, A.; Kralj-Iglič, V.; Kumar, P. B. S. Effects of Counterion Size on the Attraction between Similarly Charged Surfaces. *J. Chem. Phys.* **2010**, *133*, 204901.

(79) Ravindran, S.; Wu, J. Z. Ion Size Effect on Colloidal Forces within the Primitive Model. *Condens. Matter Phys.* **2005**, *8*, 377−388.

(80) Meng, W.; Timsina, R.; Bull, A.; Andresen, K.; Qiu, X. Additive Modulation of DNA-DNA Interactions by Interstitial Ions. *Biophys. J.* **2020**, *118*, 3019−3025.

(81) Meyer, S.; Delville, A. (N,V,T) Monte Carlo Study of the Electrostatic Forces between Charged Lamellae: Influence of Surface Charge Localization. *Langmuir* **2001**, *17*, 7433−7438.

(82) Derbenev, I. N.; Filippov, A. V.; Stace, A. J.; Besley, E. Electrostatic Interactions between Spheroidal Dielectric Particles. *J. Chem. Phys.* **2020**, *152*, 024121.

(83) Misra, R. P.; de Souza, J. P.; Blankschtein, D.; Bazant, M. Z. Theory of Surface Forces in Multivalent Electrolytes. *Langmuir* **2019**, *35*, 11550−11565.

(84) Zhang, X.; Zhang, J. S.; Shi, Y. Z.; Zhu, X. L.; Tan, Z. J. Potential of Mean Force between Like-Charged Nanoparticles: Many-Body Effect. *Sci. Rep.* **2016**, *6*, 23434.

(85) Salerno, K. M.; Frischknecht, A. L.; Stevens, M. J. Charged Nanoparticle Attraction in Multivalent Salt Solution: A Classical-Fluids Density Functional Theory and Molecular Dynamics Study. *J. Phys. Chem. B* **2016**, *120*, 5927−5937.

(86) Tan, Z.-J.; Chen, S.-J. Electrostatic Correlations and Fluctuations for Ion Binding to a Finite Length Polyelectrolyte. *J. Chem. Phys.* **2005**, *122*, 044903.

(87) Nguyen, T. T.; Grosberg, A. Y.; Shklovskii, B. I. Macroions in Salty Water with Multivalent Ions: Giant Inversion of Charge. *Phys. Rev. Lett.* **2000**, *85*, 1568−1571.

(88) Lindemann, F. A. The Calculation of Molecular Vibration Frequency. *Z. Phys.* **1910**, *11*, 609−612.

(89) Truskett, T. M.; Torquato, S.; Sastry, S.; Debenedetti, P. G.; Stillinger, F. H. Structural Precursor to Freezing in the Hard-Disk and Hard-Sphere Systems. *Phys. Rev. E* **1998**, *58*, 3083−3088.

(90) Zhou, Y.; Karplus, M.; Ball, K. D.; Berry, R. S. The Distance Fluctuation Criterion for Melting: Comparison of Square-Well and Morse Potential Models for Clusters and Homopolymers. *J. Chem. Phys.* **2002**, *116*, 2323−2329.

(91) Kanduč, M.; Naji, A.; Forsman, J.; Podgornik, R. Attraction between Neutral Dielectrics Mediated by Multivalent Ions in an Asymmetric Ionic Fluid. *J. Chem. Phys.* **2012**, *137*, 174704.

(92) Naji, A.; Kanduc, M.; Forsman, J.; Podgornik, R. Perspective: Coulomb Fluids – Weak Coupling, Strong Coupling, in between and Beyond. *J. Chem. Phys.* **2013**, *139*, 150901.

(93) Gan, Z.; Xing, X.; Xu, Z. Effects of Image Charges, Interfacial Charge Discreteness, and Surface Roughness on the Zeta Potential of Spherical Electric Double Layers. *J. Chem. Phys.* **2012**, *137*, 034708.

(94) Kanduč, M.; Naji, A.; Forsman, J.; Podgornik, R. Dressed Counterions: Polyvalent and Monovalent Ions at Charged Dielectric Interfaces. *Phys. Rev. E* **2011**, *84*, 011502.

(95) Kanduc, M.; Naji, A.; Forsman, J.; Podgornik, R. Dressed Counterions: Strong Electrostatic Coupling in the Presence of Salt. *J. Chem. Phys.* **2010**, *132*, 124701.

(96) Metropolis, N.; Rosenbluth, A. W.; Rosenbluth, M. N.; Teller, A. H.; Teller, E. Equation of State Calculations by Fast Computing Machines. *J. Chem. Phys.* **1953**, *21*, 1087−1092.

(97) Angelescu, D. G.; Linse, P. Monte Carlo Simulation of the Mean Force between Two Like-Charged Macroions with Simple 1:3 Salt Added. *Langmuir* **2003**, *19*, 9661−9668.